

INVESTIGATION OF BORONIZATION IN GLOBUS-M TOKAMAK AND GAS-FILLED DETECTORS USING THE ELECTROSTATIC ACCELERATOR BEAMS

V.M. Lebedev, A.G. Krivshich, V.A. Smolin, B.B. Tokarev, E.I. Terukov¹⁾, V.K. Gusev¹⁾

¹⁾ *Ioffe Physical-Technical Institute of RAS, St.-Petersburg*

At PNPI there is a Van de Graaf electrostatic accelerator with the energy of 1.5 MeV. The accelerator was used for a wide program of fundamental research (nuclear physics, physics of solids, films and surface semiconductors) as well as for technical and applied investigations (new materials, nuclear detectors, physical installations). At this accelerator the nuclear physics techniques of material research are used. They include a Rutherford backscattering spectrometry and a nuclear reaction analysis [1]. These techniques are nondestructive, high sensitive and precise.

The main results of investigations at this accelerator for past 5 years are presented in this article. They include:

- study of vacuum vessel boronization in Globus-M Tokamak,
- aging investigations (using nuclear microanalysis) of gas-filled particle detectors proposed for experiments at the Large Hadron Collider (LHC).

1. Study of vacuum vessel boronization in Globus-M Tokamak

1.1. Introduction

At Ioffe Physical-Technical Institute of RAS there is Globus-M Tokamak. Globus-M is a spherical small aspect ratio A tokamak (plasma major radius $R = 0.36$ m, minor radius $a = 0.24$ m, $A = R/a = 1.5$, toroidal magnetic field 0.1–0.6 T, plasma current up to 0.36 MA) presently operating in Ohmic heating regime [2, 3]. The first experiments were performed in the vacuum vessel with stainless steel limiters. Later on the vessel inner cylinder and partly the poloidal limiters were protected with graphite tiles.

The effective way to reduce the impurity contamination in tokamak plasma is the coating of the first wall with boron-carbon films. In the Globus-M experiment the boron-carbon film was deposited on the vacuum vessel inner surface in glow discharge (GD) in the mixture of helium and carboran $C_2B_{10}H_{12}$. The essential advantages of this method are the low cost and the simplicity of implementation. The carboran is the non-toxic and non-explosive substance. It is a powder at the room temperature, which is intensively evaporated at the temperature higher than 40°C.

The first boronization of the vacuum vessel was performed at a low percentage of carboran. The carboran vapor pressure was less than 10% of He pressure in glow discharge applied during 30 minutes. However, this procedure led to significant reduction of hydrogen recycling and to 20% increase of plasma current at the same loop voltage waveform. Then the Boron/Carbon films were deposited on the substrates from different materials in a high frequency glow discharge out of the Globus-M vacuum vessel and their properties were studied in details. The last boronization in the Globus-M was carried out at the essentially lower helium to carboran vapor pressure ratio in the range 3/1 – 5/1. After the boronization the analysis of the spatial distribution and the structure of the deposited film have been undertaken. For this purpose silicon probes (plates of approximately 1 cm² area) were placed in 16 points on the vessel inner surface and the graphite limiters.

1.2. Experiment

The Globus-M vacuum vessel is an all-welded stainless steel construction of ~ 1 m³ inner volume. The vessel plan view is shown in Fig. 1, the contour of the vertical cross-section is depicted in Fig. 2. Figures 1–2 show also the position of silicon plates located in four sections along the torus.

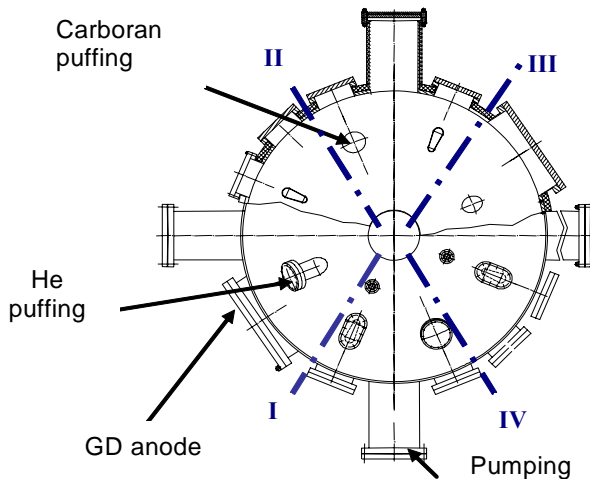


Fig. 1. Vacuum vessel plan view showing position of He and carboran puffing and CD electrode. I, II, III, IV – sections for silicon plates positioning

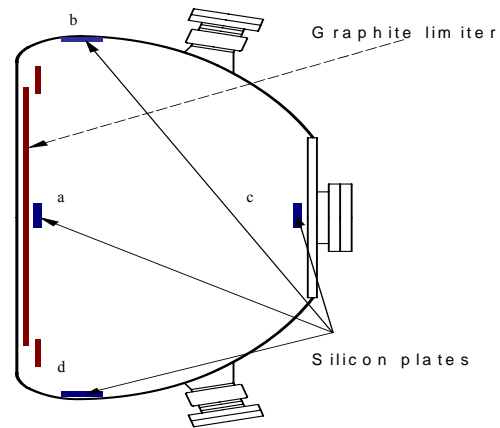


Fig. 2. Vacuum vessel cross-section showing the position of silicon plates and graphite limiter

The routine procedure of the vessel conditioning includes the bake-out at the temperature up to 200°C and the glow discharge cleaning in hydrogen and noble gases. The glow discharge voltage is applied between the single electrode (anode) and the earthed vessel. The electrode of 20 mm diameter is positioned in the tokamak middle plane (see Fig. 1). The parameters of the vessel and the glow discharge characteristics are shown in Table 1. The helium pressure was provided by the piezoelectric valve. The carboran was evaporated by heating the ampoule containing the carboran powder. The steady state temperature of 45°–48°C was sufficient to sustain the required pressure.

Table 1

The vessel parameters and glow discharge characteristics of the Globus-M Tokamak

Diameter of outer wall	1260 mm	Glow discharge voltage	300 V
Diameter of graphite limiter	252 mm	Current density	30 $\mu\text{A}/\text{cm}^2$
Vertical axis of torus	1.094 m	Gas pressure	0.2 Pa
Vessel volume	1.05 m ³	He to carboran pressure ratio	3/1 – 5/1
Inner surface area	5.7 m ²		

1.3. Results

First detailed study of carboran film properties was performed for the films deposited on the silicon, quartz and glass plates in 40 MHz He or Ar glow discharge in a small laboratory device (the distance between electrodes was 35 mm). The basic results can be summarized as follows.

The deposition rate decreased when the substrate temperature rose in the range of 20°–100°C. The films had the amorphous structure.

The Boron/Carbon ratio was determined from the nuclear reactions analysis (NRA) with deuterons. Figure 3 shows the energy spectra of protons and α -particles originated in the reactions of 1 MeV deuterons with nuclei of carbon and boron isotopes. The B/C ratio in the deposited films was determined by integrating the peaks of $^{10}\text{B}(d,\alpha)^8\text{Be}$ and $^{12}\text{C}(d,p)^{13}\text{C}$ reactions [2, 3] and appeared to be about 48/52 in percents.

The content of hydrogen (result of infra-red spectrum analysis) reached 40–50% at the room temperature and could be reduced by annealing at a higher temperature.

The characteristic values of the specific resistance is equal approximately to 10^6 Ohm·cm at the room temperature and $\sim 10^5$ Ohm·cm at the temperature of 100°C. The films are transparent in the visible range. After the vessel boronization with a small fraction of carboran vapor pressure (less than 10% of He pressure)

the subsequent analysis of silicon plates revealed a formation of thin films with a typical thickness of 100 Å. The film had an amorphous structure, but the content of boron did not exceed 4%. After 200 plasma shots with the plasma current of 150 kA accompanied by routine glow discharge cleaning in helium during 70 hours the amorphous structure transformed to the diamond-like one. It is remarkable that the hydrogen in the film was practically absent.

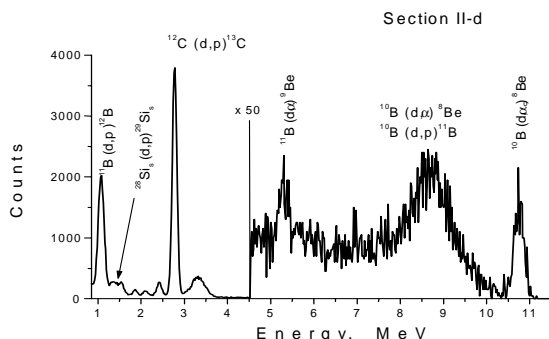


Fig. 3. Energy spectrum of protons and α -particles originated in the reactions of 1 MeV deuteron beam with carbon and boron isotopes in the deposited film. Angle of observation is 135° relatively to the beam

More detailed analysis was undertaken after the boronization with the ratio of helium to carboran pressure in the range 3/1 – 5/1 during 1.5 hour. The boronization was followed by a short experimental series from 80 plasma shots with plasma current of 200 kA and 12 hours of glow discharge cleaning in helium. The distribution of the film thickness deposited on silicon plates in different points of the vessel is shown in Table 2. The plates numbering is given according to Figs. 1–2.

The film composition in the cross-section II (Fig. 1) was studied by means of nuclear reaction analysis (NRA) and Rutherford backscattering spectrometry (RBS) at the PNPI electrostatic accelerator. The content of iron was obtained from the RBS spectrum of deuterons. These results are presented in Table 3.

Table 2

Film thickness on silicon plates in the Globus-M Tokamak				
Film thickness, μm				
Position	a	b	c	d
I	-	1	0.5	0.4
II	0.03	0.65	0.1	0.3
III	-	0.3	0.3	0.3
IV	-	0.3	1.2	0.4

Table 3

Film composition in cross-section II of the Globus-M Tokamak	
Substrate	Composition of film
II-a	$\text{B}_{0.32 \pm 0.02} \text{C}_{0.52} \text{Fe}_{0.16}$
II-b	$\text{B}_{0.01} \text{C}_{0.52 \pm 0.02} \text{Fe}_{0.43}$
II-c	$\text{B}_{0.27 \pm 0.02} \text{C}_{0.55} \text{Fe}_{0.18}$
II-d	$\text{B}_{0.43 \pm 0.02} \text{C}_{0.47} \text{Fe}_{0.10}$

1.4. Conclusion

The described procedure of Globus-M vessel boronization leads to a formation of the amorphous boron-carbon film with a typical B/C ratio of 3/4–3/5. The film thickness varies within a factor of 4 along the vessel surface. No obvious correlation between the film thickness and the position of the glow discharge electrode and the gas puffing ports was observed. The physical properties of the B-C coating deposited in DC glow discharge on the vessel surface are similar to properties of the films obtained in 40 MHz discharge. The appearance of iron in the film structure can be explained by a sputtering of the vessel material during boronization and the tokamak routine operation. Thinner films have a lower content of boron. The tokamak operation (plasma shots and routine glow discharge cleaning) leads to a significant reduction of hydrogen content in the boron-carbon films.

2. Aging investigations of gas-filled particle detectors by means of Nuclear Reaction Analysis

2.1. Introduction

Some time ago it was demonstrated that the method of Nuclear Reaction Analysis (NRA) is very effective for investigation of the aging effects in the gas-filled detectors [4–6] operated under high accumulated dose. This technique is particularly efficient in quantitative evaluation of the light elements (oxygen, carbon, nitrogen, fluorine, *etc.*) presence in the gold coating of the anode wire. The NRA method is also adequate for determining light element distribution with a depth measurement over a range of more than 1 μm .

Such data are especially important in studies of gas discharge avalanche plasmas because they are a starting point for most of the aging processes in the gas filled detectors. Wire aging is an extremely complex chemical process. To obtain a general picture of wire aging, it is necessary to identify the dominant processes occurring in gas avalanches, which result in the production of active chemical species (radicals, ions, *etc.*). The avalanche environment is plasma of ions and neutral radicals, and thus the wire aging process should be studied in the framework of plasma chemistry. The most important plasma-chemical reactions for the gas mixtures ($\text{Ar}/\text{CO}_2/\text{CF}_4$ and $\text{Xe}/\text{CO}_2/\text{CF}_4$) produce many different active species including oxygen and fluorine [4–7].

Application of the NRA method in our aging investigations gave us a reliable confirmation of the oxygen key role in the wire-swelling mechanism and demonstrated the kinetics of oxygen transport into the depth of the gold coating of the anode tungsten wire [5–7]. Active elements, including radicals, penetrate through the already opened cracks in the gold layer and react directly with the wire tungsten. Finally, this causes a swelling of the tungsten in the wire and, as a consequence, forces break of the gold coating produced within the wire.

But initial imperfections in the gold crystallite structure, which can increase and develop under the influence of sustained irradiation and etching of the gold, can provide favorable conditions for active oxygen with broken bounds, and even for more complicated chemical radicals, to penetrate into the tungsten. Etching strongly attacks defects in the gold coating and results in its extension. It should be noted that etching is a dangerous process which can open a direct path for the active oxygen to the tungsten surface of the wire. Special interest for our gas mixture are two chemical agents which determine possible gold etching: fluorine and xenon-fluorine XeF_n ($n = 2, 4, 6$) compounds. These agents are strong oxidizers and may interact with the gold causing etching. So, in order to understand the aging (including the wire swelling) mechanism in more detail, it was principally important to develop the NRA method for investigation of fluorine distribution in the anode wires. In case of success we would get the method allowing to perform the detection and quantitative evaluation of all light elements (oxygen, carbon, fluorine, nitrogen) which are coming from gas mixtures used in gaseous detectors and concentrated in electrodes.

2.2. NRA technique

For the detection and quantitative evaluation of the fluorine content as a function of depth in the gold, the nuclear reaction $^{19}\text{F}(p,\alpha)^{16}\text{O}$ has been applied [5, 8]. The reaction is exothermic and thus the exiting α -particles have higher energies ($E_\alpha = 7$ MeV) in compare with the incoming protons ($E_p = 1.25$ MeV) which are scattered on the target. This allows us to absorb completely the beam ions with a few microns of aluminum foil placed in front of the semiconductor detector, which is used for detection of the final state particles. Due to the Coulomb barrier the energy of the bombarding protons is not sufficient for nuclear interaction with higher atomic number elements (such as Al, Au, W). Hence, the α -particles produced in the interaction with fluorine atoms are detected practically without background.

The NRA was carried out at the PNPI electrostatic accelerator. The frame with investigated wire was fastened to the target apparatus of a vacuum chamber. A proton beam of 1.25 MeV was used. The diameter of the beam spot on the wire was about 4 mm. The beam current through the wire was about 3–5 nA. The heat consumption of the irradiated wire was 0.01–0.02 W/cm. The number of protons, which passed the wire, was evaluated with the current integrator. α -particles were detected by a surface-barrier Si(Au) detector positioned at an angle of $\theta = 135^\circ$ relatively to the beam axis.

To measure the distribution of fluorine along the wire the target was scanned with the beam. The method is based on the analysis of the energy spectra of emitted particles and makes it possible to determine a light element concentration profile. Schematics and nomenclature for the (p,α) nuclear reaction process in a sample-target and the reconstruction of the resulting energy spectrum are presented in Fig. 4. The energy spectrum of the α -particles produced by the (p,α) -reactions at a constant energy of protons was measured using a semiconductor detector. Back-scattered protons are filtered out using a thin (6 mg/cm^2) aluminum foil.

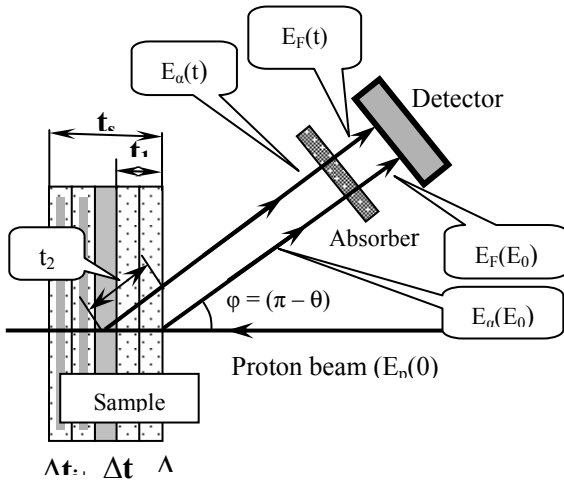


Fig. 4. Schematics and nomenclature for the (p,α) nuclear reaction process in sample

The energy of the detected α -particle resulting from the reactions at a depth t depends on the relation between the beam particle energy and the path traveled by the emitted particles. A reaction, which takes place near the surface of the specimen, will yield α -particles with higher energy than a reaction which occurs at a greater depth.

The *energy-depth* relation may be deduced from the fact that the measured energy of α -particle produced at the depth t depends on the energy loss of protons reaching the depth t and the energy loss of α -particle in the

traversing the sample before it reaches the detector. To calculate this relation, a sample is sliced on thin layers with the thickness of Δt_i (Fig. 4). The energy of protons $E_p(t)$ with incident energy $E_p(0)$ at the depth t_1 is given by the equation:

$$E_p(t) = E_p(0) - \int_0^{t_1} |S_p(t)| dt,$$

where $S_p(t)$ is a stopping power of substance for protons, t_1 is a path length of protons in the target.

The energy $E_\alpha(E_p)$ of α -particle resulting from a reaction (p,α) is given by the well-known expression:

$$E_\alpha(E_p(t)) = M_\alpha M_p E_p \{ 2\cos^2\theta + B + 2\cos\theta [\cos^2\theta + B]^{1/2} \} / (M + M_\alpha)^2,$$

where θ is the angle between the beam direction and the detector direction; M_p , M_α , M – the masses of incident particle, outgoing particle and final nucleus; $B = M(M + M_\alpha)(Q_R/E_p - M_p/M + 1)/(M_\alpha M_p)$.

The energy of α -particle in the detector $E_F(t)$ is given by the equation below:

$$E_F(t) = E_\alpha(E_p(t)) - \int_0^{t_2} |S_\alpha(t)| dt - \int_0^{t_{Al}} |S_\alpha(t_{Al})| dt,$$

where $S_\alpha(t)$ is the stopping power of substance for α -particles; $t_2 = t_1/\cos\theta$ is the path length of α -particles in the target; t_{Al} is the thickness of the aluminum foil-absorber.

Using tabulated stopping power data, the $E_F(t)$ dependence can be calculated from these equations. This approximation appears to be quite reasonable if we take into account that the energy loss of particles is relatively small compared with their initial energy and the stopping powers have a linear dependence on the energy and vary less than 15% over the relevant energy ranges: 1.0–1.25 MeV for protons, 4.0–7.0 MeV for α -particles [4, 8]. In this case the energy scale can be converted into a linear depth scale:

$$E_F(t) = E_F(E_0) - G_{NR} t,$$

where $G_{NR} = (\partial E_\alpha / \partial E_p) S_p + S_\alpha / \cos\theta$. G_{NR} is an effective energy loss related to single length. The G_{NR} depends on energy losses of α -particles and protons, reaction kinematics, geometry of experiment, and elemental composition of investigated sample. $G_{NR} = 380 \text{ keV/mg/cm}^2$ for an investigated wire.

As shown in Fig. 4, we sliced the investigated sample per thin layers to provide the calculation. The thickness Δt_i connects with energy interval ΔE_i of experimental spectrum by equation $\Delta t_i = \Delta E_i / G_{NR}$.

The energy spectrum $Y(E_F)$ of the detected α -particles is given by the equation:

$$Y(E_F(t)) dE_F = C(t) \cdot I \cdot \sigma(E_p(t)) \cdot \Delta\Omega \cdot dt,$$

where $C(t)$ is the concentration profile of fluorine, *i.e.* the number of element atoms per cm^3 at the depth t ; I is the number of incident particles; $\sigma(E_p(t))$ is the differential cross section for the angle θ ; $\Delta\Omega$ is the solid angle of a particle detection.

The sensitivity of NRA technique for the fluorine concentration measurements is about 1×10^{16} at/cm². An accuracy of the element concentration measurements is better than 5%. The thickness of the investigated layer depends on the range of particles in a sample (for protons and α -particles) and in the absorber (for α -particles). The available thickness of the gold or tungsten, which may be obtained from calculations, does not exceed 2–4 μm .

2.3. Results

The results obtained by the NRA analysis for different points along the wire are shown in Figs. 5-6. The fluorine concentration along the anode wire and their depth distributions have been measured for Ar(80%)+CO₂(10%)+CF₄(10%) gas mixture under the total accumulated charge up to 1.8 C/cm. Diameter of the gold plated wire is equal to 35 μm . The degradation test of the straw drift-tube (ATLAS TRT) was carried out using a 2 Ci ⁹⁰Sr β -source.

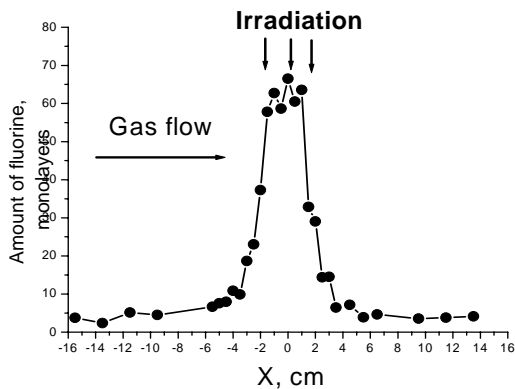


Fig. 5. The distribution of fluorine content along the irradiated wire. The element content of 1 monolayer is equal to 10^{15} at/cm²

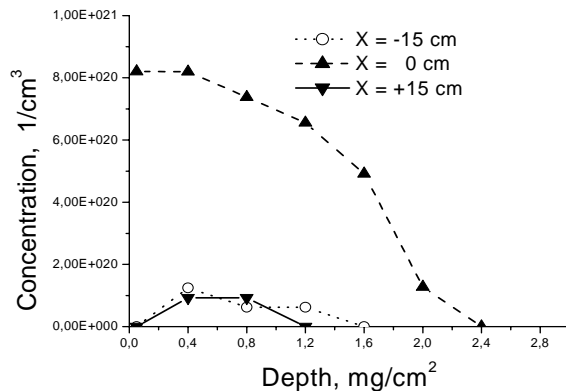


Fig. 6. The distribution of fluorine concentration as a function of depth into gold layer for different points along the irradiated wire

As one can see, after irradiation of the wires the amount of fluorine is noticeably increases. In the center of the irradiated zone the total amount of fluorine collected in gold has increased up to 15 times in comparison to the non-irradiated wire. Moreover, the maximum value of the fluorine peak concentration increased up to 10 times, reaching a value of 8×10^{20} at/cm³. In irradiated places of the wire the depth of the fluorine penetration is up to 2.5 mg/cm^2 . There is a direct correlation between the distribution of fluorine, oxygen and carbon concentrations along the wire and the beam irradiation profile (Fig. 7 and Table 4). It is shown that the fluorine concentration profile is correlated with changes of the wire diameter (increasing in the irradiation zone) and a gas gain (decreasing in the irradiation zone). For the detection and quantitative evaluation of the oxygen and carbon content as a function of depth in gold, the following nuclear reactions with deuterons in the energy range of 0.7–1.1 MeV have been applied: $^{12}\text{C}(d,p)^{13}\text{C}$ and $^{16}\text{O}(d,p)^{17}\text{O}$ [4].

Dependence of element content, anode wire diameter and gas gain for different points along the wire.
Center of irradiated area corresponds to $X=0$ cm. Total accumulated charge is about 1.8 C/cm

Distance along the straw	Content of elements in monolayers			Gas gain, relative units	Wire diameter, μm
	Fluorine	Oxygen	Carbon		
-15 cm	4-5	50	25	1	35
0 cm	70	600	270	0.74	36.2
+15 cm	5-6	70	35	1	35

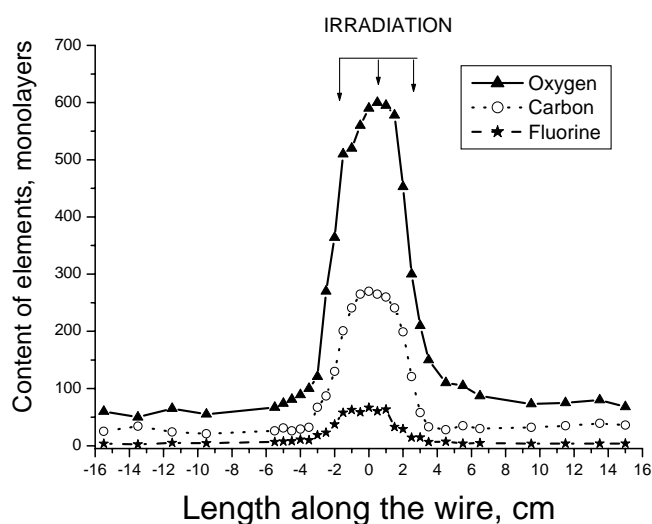


Fig. 7. The distribution of oxygen, carbon and fluorine content along the irradiated wire

2.4. Conclusion

The method of Nuclear Reaction Analysis (NRA) has been successfully developed at PNPI for investigation of the aging effects in the gas-filled detectors caused by fluorine and fluorine-containing compounds.

This method looks very promising and offers unique possibilities due to its high sensitivity, the fact that no etching is needed. The NRA method permits to investigate the lateral and depth distributions of the fluorine in samples.

Measurements of the oxygen, carbon and fluorine concentrations in the gold coating of the tungsten wire can provide an excellent method to compare the aging resistance of different wires which are intended to be used in the gas-filled detectors under high-accumulated dose.

References

1. V.M. Lebedev, V.A. Smolin and B.B. Tokarev, Preprint PNPI-2609, Gatchina, 2005. 24 p.
2. A.S. Ananiev, V.M. Lebedev, E.I. Terukov *et al.*, Semiconductors, **36**, 941 (2002).
3. N.V. Sakharov, V.K. Gusev, V.M. Lebedev, E.I. Terukov *et al.*, in *Proceedings of the 29th Conference on Plasma Physics and Controlled Fusion* (Montreux, Switzerland, 17 – 21 June 2002), p - 5.078 (2002).
4. G. Gavrilov, A. Krivshich and V. Lebedev, Nucl. Instr. Meth. A **515**, 108 (2003).
5. T. Ferguson, A. Krivshich, V. Lebedev *et al.*, Nucl. Instr. Meth., A **483**, 698 (2002).
6. T. Ferguson, A. Krivshich, V. Lebedev *et al.*, Nucl. Instr. Meth. A **515**, 266 (2003).
7. V.M. Lebedev, A.G. Krivshich and V.A. Smolin, Questions of Atomic Science and Technique, series: physics of nuclear reactors, **2**, 48 (2006).
8. V.M. Lebedev, A.G. Krivshich and A.N. Tatarinsev, Preprint PNPI-2616, Gatchina. 2005. 22 p.